18

COO-1726-31

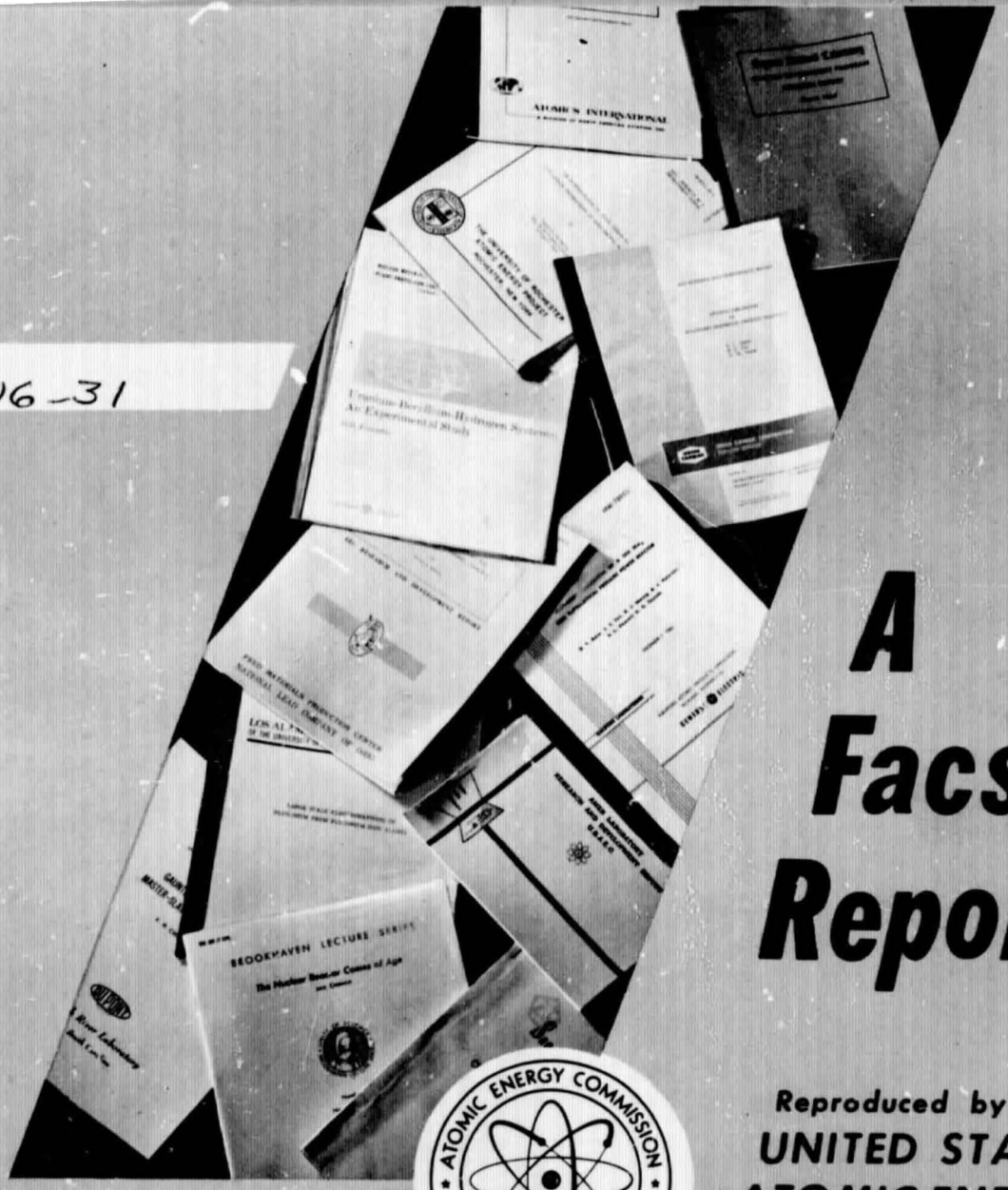

A Facsimile Report

Reproduced by
UNITED STATES
ATOMIC ENERGY COMMISSION
Division of Technical Information
P.O. Box 62 Oak Ridge, Tennessee 37830

SQT-62784

COO-1746-31

Determination of the E2/M1 Multipole Mixing Ratios of the Gamma Transitions in Cd^{110} *

K. S. Krane† and R. M. Steffen

Department of Physics, Purdue University
Lafayette, Indiana 47907

(Received)

* Work supported by the U. S. Atomic Energy Commission under Contract No. AT(11-1)1746 (Chicago Operations Office).

† NASA - Fellow

ABSTRACT

The multipole character and E2/M1 mixing ratios of all gamma transitions following the decay of Ag^{110m} to Cd^{110} have been determined by measuring the 1-2, 1-3, and 1-4 directional correlations using two 30cc coaxial Ge(Li) detectors in conjunction with a multichannel coincidence gating system. The analysis of the data clearly demonstrated the necessity for careful investigations of the effects of the Compton background on directional correlation measurements using Ge(Li) detectors. The directional correlation functions for mixed gamma-gamma cascades are given in terms of explicitly defined reduced matrix elements and their ratios $\delta(\gamma_n)$. The analysis of the 25 measured directional correlations yielded a consistent set of E2/M1 mixing ratios for all mixed multipole transitions. The E2/M1 amplitude ratios $\delta(\gamma_n) = \langle I_{n+1} \| \underset{\sim}{j}_N \underset{\sim}{A}_2^E \| I_n \rangle / \langle I_{n+1} \| \underset{\sim}{j}_N \underset{\sim}{A}_1^M \| I_n \rangle$ for the Cd^{110} gamma rays are (energies are in keV): $\delta(447) = -0.45 \pm 0.20$, $\delta(620) = -0.80 \pm 0.50$, $\delta(678) = -0.25 \pm 0.20$, $\delta(687) = -1.1 \,^{+\,0.8}_{-\,0.4}$, $\delta(707) = -1.0 \pm 0.3$, $\delta(818) = -1.20 \pm 0.15$, $\delta(1384) = -0.37 \pm 0.03$, $\delta(1505) = -0.55 \pm 0.10$. In terms of the multipole moments $\langle I_{n+1} \| \mathcal{M}(\pi L) \| I_n \rangle$ of Bohr and Mottelson the E2/M1 moment ratios $\Delta = \langle I_{n+1} \| \mathcal{M}(E2) \| I_n \rangle / \langle I_{n+1} \| \mathcal{M}(M1) \| I_n \rangle$ in natural units ($\hbar = m = c = 1$) are: $\Delta(447) = 3.0 \pm 1.3$, $\Delta(620) = -3.8 \pm 2.4$, $\Delta(678) = -1.09 \pm 0.88$, $\Delta(687) = -4.7 \,^{+\,3.4}_{-\,1.7}$, $\Delta(707) = -4.2 \pm 1.3$, $\Delta(818) = -4.3 \pm 0.5$, $\Delta(1384) = -0.79 \pm 0.06$, $\Delta(1505) = -1.08 \pm 0.20$.

I. INTRODUCTION

The excited states of even-even nuclei in the mass region $100 < A < 140$ have been interpreted as collective vibrational oscillations about a spherical equilibrium shape of the nuclear surface.[1] The complete understanding of this class of nuclear excitations, however, is still far from being satisfactory.

In a phenomenological description the nuclear vibrations are considered harmonic oscillations of small amplitude. This model predicts 2^+ first excited states of energy $E_1 = \hbar\omega$ (one-phonon states) and a degenerate set of 0^+, 2^+ and 4^+ second excited states of energy $E_2 = 2\hbar\omega$ (two-phonon states). A displaced harmonic oscillator potential[2] partially removes the degeneracy of the 0^+, 2^+, 4^+ triplet and the ratio E_2/E_1 can increase from 2.0 to 2.5. These predictions are in agreement with experimental data. Within the framework of the harmonic vibrational model the excited states decay by emission of pure E2 radiation; M1 radiation is strictly forbidden. Also, the cross-over E2 transition from the two-phonon $2^{+'}$ state to the 0^+ ground state is forbidden. The observation of this cross-over transition in most of the nuclei of the $100 < A < 140$ region and the observation of appreciable M1 admixture in the transitions from the two-phonon $2^{+'}$ to the one-phonon 2^+ excited state are not in accord with the harmonic vibration model. Futhermore, pure vibrational (pure phonon) states have a static quadrupole moment that is zero, because the quadrupole moment operator is a linear combination of a creation and annihilation operator of a phonon and thus the diagonal matrix elements vanish with respect to states that have a definite number of phonons. The observation of the reorientation effect in Coulomb excitation[3] has clearly revealed that the first excited states of the so-called vibrational nuclei have quadrupole moments of the order of ~ 0.5 b, clearly indicating that the harmonic vibration model is inadequate.

The interpretation of the first excited state in terms of a superposition of the one- and two-phonon harmonic vibrational 2^+ states can explain the observed quadrupole moments[4] but fails to account for the M1 transitions. This mixed-phonon state model corresponds, in essence, to an anharmonic oscillator model and the problem of the anharmonicity has been studied from different points of view based on a microscopic description of the problem. Bes[5] et al. have treated some of the important particle degrees of freedom, and Sorensen[6] has taken into account that the quasi-bosons formed by the combination of Fermion operators do not possess the properties of ideal bosons. Higher random-phase-approximation calculations using the pairing plus quadrupole model of the residual interactions have been performed by Tamura and Udagawa[4] and by Sorensen[7]. However, the computed quadrupole moments of the first excited 2^+ states are too small ($Q \sim -0.08$ b).

It seems that the vibrational aspects play a major role in the description of the gross structure of these nuclei, at least for the first few excited states, but that an understanding of the higher excited states and the quantitative aspects of the structure of the lower excited states requires a more detailed microscopic description. In any case, the causes of the anharmonicity in the "vibrational" description are not clear[8]. The interplay between the vibrational modes and the two quasi-particle states is probably of major importance.

Korolev[9] considered the M1 and E2 transition probabilities in "vibrational" nuclei on the basis of a simple extra-pair model in which the nucleus is treated as a magic core plus one or more zero-spin nucleon pairs, which interact with the core and excite collective degrees of freedom. The nuclear excitations are treated as excitations of a pair in a potential well plus phonon excitations of

the core.

The most successful approach to a better understanding of the structure of the "vibrational" nuclei has been made by Kumar and Baranger[10]. They explore in detail the potential energy surfaces and mass parameters of the quadrupole motion on the basis of the pairing-plus quadrupole force and then solve the Bohr-Hamiltonian. The success of these calculations, which have been performed for the mass region $184 < A < 196$, is remarkable. The predicted quadrupole deformations, as well as the g-factors and the E2/M1 multipole mixing ratios, agree surprisingly well with the available experimental data[11]. Unfortunately, no extensive calculations of the Kumar-Baranger type have been made as yet for the mass region $100 < A < 140$.

The present investigation of the relative amplitude of the M1 transitions in a typical "vibrational" nuclei, i.e., Cd^{110} was undertaken in order to have available accurate experimental data for comparison with future calculations of the Kumar-Baranger type.

The E2/M1 multipole mixing ratios of the Cd^{110} gamma transitions were determined on the basis of γ-γ directional correlation measurements performed with high resolution Ge(Li) detectors. The multipole character of all gamma rays in Cd^{110} that follow the β-decay of Ag^{110m} has been determined and the results are presented in terms of ratios of explicitly defined reduced matrix elements.

II. THE LEVEL STRUCTURE OF CD^{110}

The decay of Ag^{110m} to Cd^{110} has been studied by a number of investigators[12-22]. Early studies of the decay scheme by directional correlation techniques[12-15,19] and extensive studies of beta rays and internal conversion electrons[16-18,20] have resulted in a well-established level scheme of Cd^{110}. The use of solid-state Ge(Li) detectors has permitted an accurate determination of the energies and intensities of the Cd^{110} gamma transitions[21], and attempts have been made to study quadrupole, octupole, and hexa-decupole vibrational states by inelastic proton scattering[22].

The first two excited states of Cd^{110} (Fig. 1) show qualitatively some of the characteristic features of a "vibrational" nucleus. The ratio $E_2(2')/E_1 = 2.25$ is close to the predicted value of 2. The ratio $B(E2,2' \rightarrow 2)/B(E2,2 \rightarrow 0 = 1.08 \pm 0.29$ as measured by Milner et al.[23] is considerably smaller than the value of 2.0 as predicted by the vibrational model, but it is in good agreement with the calculations of Korolev[9] $B(E2,2' \rightarrow 2)/B(E2,2 \rightarrow 0) = 1.022$. The experimental ratio $B(E2,2' \rightarrow 0)/B(E2,2 \rightarrow 0) = 0.045 \pm 0.014$ also agrees well with 0.0355, the prediction of the Korolev model[9]. The vibrational model gives $B(E2,2' \rightarrow 0) = 0$. The branching ratio of the cross-over / cascade transitions for the decay of the two-phonon state 2' is [20,22] $T(2' \rightarrow 0)/T(2' \rightarrow 2) = 0.55 \pm 0.04$ in clear disagreement with the vibrational model which forbids a cross-over transition.

Recently a gamma radiation of 815.6 keV that is emitted following the β-decay of the Ag^{110g} and which is in coincidence with the 658 keV ground state transition has been interpreted as originating from a 0^+ excited state in Cd^{110} of 1473 keV excitation energy[24]. This interpretation would complete the two-phonon triplet in Cd^{110}.

The g-factor of the one-phonon 2^+ state is $g = 0.30 \pm 0.12$ [25] in fair agreement with the predicted value of the vibrational model, $g_{2^+} \cong Z/A = 0.44$.

The quadrupole moment of the 2^+ state has not been measured yet. It is very well possible that this quadrupole moment is small, since Cd^{110} could be in a transition region from positive to negative quadrupole moments[26]. The 2^+ states of the neighboring nuclei Pd^{110}, and Cd^{112} have quadrupole moments of $Q(Pd^{110}) = -0.45 \pm 0.15$ [27] and $Q(Cd^{112}) = +0.12 \pm 0.35$ [28]. Little is known about the structure of the higher excited states of Cd^{110}.

The increased resolution of Ge(Li) detectors over NaI scintillators has prompted a remeasurement of the directional correlations of the gamma rays emitted from the excited states of Cd^{110} following the decay of Ag^{110m}. Internal conversion studies[20] indicate that, of the fifteen gamma rays emitted, eight are expected to show mixed dipole-quadrupole multipolarity. Previously it had been possible to determine the multipole mixing ratio of only two of these transitions[19]; however, the use of Ge(Li) detectors permits an investigation of the multipole character of all gamma rays emitted.

III. DIRECTIONAL CORRELATIONS INVOLVING MIXED MULTIPOLE RADIATIONS

Since the interest in this work is concentrated on the precise determination of the multipole mixing ratios of the gamma transitions in Cd^{110} it is imperative that the analysis of the experimental data is made on the basis of well-defined expressions for the amplitude ratios of the various multipole components. In the past a comparison of the experimentally determined mixing ratios with results of nuclear model calculations was difficult since few experimentalists took the pains to express their measured results in terms of explicitly defined mixing ratios. In particular the signs of the amplitude ratios of the multipole components of the emitted radiation have been rarely defined. Furthermore, in many

theoretical papers on angular distributions and correlations of gamma radiations the gamma transition operators and hence the transition matrix elements that are used in the expressions for the angular distributions are not explicitly given[29]. A notable exception is the review paper by Rose and Brink[30], who, however, use a somewhat unusual notation for their matrix elements.

In the following we present a detailed and consistent definition of the reduced matrix elements that are used in our analysis of the data and give a comparison with the reduced multipole matrix elements of Rose and Brink[30] and with the widely used multipole moments of Bohr and Mottelson[31,32].

The transition matrix element for the <u>emission</u> of an electromagnetic multipole radiation πL ($\pi = E$ or $\pi = M$ for electric or magnetic multipole radiation, respectively) from an initial nuclear state $|I_i m_i\rangle$ to a final nuclear state $|I_f m_f\rangle$ is $\langle I_f m_f | \underset{\sim}{j}_N \underset{\sim}{A}_{LM}^{(\pi)*} | I_i m_i \rangle$ where $\underset{\sim}{j}_N$ is the nuclear current operator and $\underset{\sim}{A}_{LM}^{(\pi)}$ are the multipole fields in the form: (in units $\hbar = m = c = 1$)

$$\underset{\sim}{A}_{LM}^{(M)}(k, \underset{\sim}{r}) = i^L \frac{\underset{\sim}{L}}{[L(L+1)]^{\frac{1}{2}}} j_L(kr)\, Y_{LM}(\hat{r}) \tag{1a}$$

$$\underset{\sim}{A}_{LM}^{(E)}(k, \underset{\sim}{r}) = \frac{i^L}{k} \frac{\nabla \times \underset{\sim}{L}}{[L(L+1)]^{\frac{1}{2}}} j_L(kr)\, Y_{LM}(\hat{r}) \tag{1b}$$

The $j_L(kr)$ are spherical Bessel functions and k is the transition energy (in units mc^2). The vector fields (1) satisfy the equation:

$$\underset{\sim}{A}_{LM}^{(\pi)*} = (-1)^{L-M+1}\, \underset{\sim}{A}_{L-M}^{(\pi)} \tag{2}$$

Hence the interaction operator $\underset{\sim}{j}_N \underset{\sim}{A}_{LM}^{(\pi)}$ is related to its Hermitian adjoint by $(\underset{\sim}{j}_N \underset{\sim}{A}_{LM}^{(\pi)})^\dagger = (-1)^{L-M+1} (\underset{\sim}{j}_N \underset{\sim}{A}_{L-M}^{(\pi)})$. For local nuclear forces the nuclear current operator $\underset{\sim}{j}_N$ is proportional to the nuclear momentum and spin

operators $\underset{\sim}{p}$ and $\underset{\sim}{\sigma}$, respectively, which transform under the time-reversal operation T as $T\,\underset{\sim}{p}\,T^{-1} = -\underset{\sim}{p}$ and $T\,\underset{\sim}{\sigma}\,T^{-1} = -\underset{\sim}{\sigma}$. Hence the interaction operators $\underset{\sim}{j}_N \underset{\sim}{A}_{LM}^{(\pi)}$ transform under time-reversal according to $T(\underset{\sim}{j}_N \underset{\sim}{A}_{LM}^{(\pi)})T^{-1} = (-1)^{L-M}(\underset{\sim}{j}_N \underset{\sim}{A}_{L-M}^{(\pi)})$. If the nuclear eigenstates $|Im\rangle$ are chosen with their phases such that $T|Im\rangle = (-1)^{I-m}|I-m\rangle$, which is always possible, the matrix elements $\langle I_f m_f|\underset{\sim}{j}_N \underset{\sim}{A}_{LM}^{(\pi)}|I_i m_i\rangle$ are real.

The reduced gamma emission matrix elements $\langle I_f\|\underset{\sim}{j}_N \underset{\sim}{A}_L^{(\pi)}\|I_i\rangle$ are defined by the Wigner-Eckart theorem:

$$\langle I_f m_f|\underset{\sim}{j}_N \underset{\sim}{A}_{LM}^{(\pi)*}|I_i m_i\rangle = (-1)^{L-M+1}\langle I_f m_f|\underset{\sim}{j}_N \underset{\sim}{A}_{L-M}^{(\pi)}|I_i m_i\rangle$$

$$= (-1)^{L-M+1}(-1)^{I_f - m_f}\begin{pmatrix} I_f & L & I_i \\ -m_f & -M & m_i \end{pmatrix}\langle I_f\|\underset{\sim}{j}_N \underset{\sim}{A}_L^{(\pi)}\|I_i\rangle \qquad (3)$$

where $\begin{pmatrix} I_f & L & I_i \\ -m_f & -M & m_i \end{pmatrix}$ is the Wigner 3-j symbol. Note that the initial states of a transition are always written on the right side in the matrix elements. Equation (3) refers to the emission of electromagnetic radiation, i.e. $E_i > E_f$.

The (real) reduced matrix elements defined in eq. (3) are related to the reduced matrix elements of Bohr and Mottelson[31] and of Alder et al.[32] by

$$\langle I_f\|\underset{\sim}{j}_N \underset{\sim}{A}_L^{(E)}\|I_i\rangle = \frac{k^L}{(2L+1)!!}\left(\frac{L+1}{L}\right)^{\frac{1}{2}}\langle I_f\|i^L \mathcal{M}(EL)\|I_i\rangle_{BM} \qquad (4a)$$

$$\langle I_f\|\underset{\sim}{j}_N \underset{\sim}{A}_L^{(M)}\|I_i\rangle = -\frac{k^L}{(2L+1)!!}\left(\frac{L+1}{L}\right)^{\frac{1}{2}}\langle I_f\|i^{L-1}\mathcal{M}(ML)\|I_i\rangle_{BM} \qquad (4b)$$

The reduced matrix elements $\langle I_f\|\underset{\sim}{j}_N \underset{\sim}{A}_L^{(\pi)}\|I_i\rangle$ are related to those of Rose and Brink[30] by:

$$\langle I_f\|\underset{\sim}{j}_N \underset{\sim}{A}_L^{(\pi)}\|I_i\rangle = -(-1)^{I_1 - I_2 + L + 1}(2\pi(2L+1))^{-\frac{1}{2}}(2I_i+1)^{\frac{1}{2}}\langle I_i\|T_L^{(\pi)}\|I_f\rangle_{RB} \qquad (5)$$

Note that in Rose and Brink's paper[30] the initial state for emission processes is always written on the left side of the interaction operator ($E_i > E_f$).

The directional correlation of two mixed multipole gamma radiations, emitted according to the scheme $I_1 \xrightarrow{\gamma_1} I_2 \xrightarrow{\gamma_2} I_3$, is given by

$$W(\theta) = \sum_\Lambda B_\Lambda(\gamma_1)\,A_\Lambda(\gamma_2)\,P_\Lambda(\cos\theta) \qquad (6)$$

where the normalized orientation coefficient $B_\Lambda(\gamma_1)$ is given by:

$$B_\Lambda(\gamma_1) = \frac{\sum_{L_1\pi_1 L_1'\pi_1'} F_\Lambda(L_1L_1'I_1I_2)\,(-1)^{L_1 - L_1'}\langle I_2\|\underset{\sim}{j}_N \underset{\sim}{A}_{L_1}^{(\pi_1)}\|I_1\rangle\langle I_2\|\underset{\sim}{j}_N \underset{\sim}{A}_{L_1'}^{(\pi_1')}\|I_1\rangle}{\sum_{L_1\pi_1}\langle I_2\|\underset{\sim}{j}_N \underset{\sim}{A}_{L_1}^{(\pi_1)}\|I_1\rangle^2} \qquad (7)$$

and the directional distribution coefficient $A_\Lambda(\gamma_2)$ is given by

$$A_\Lambda(\gamma_2) = \frac{\sum_{L_2\pi_2 L_2'\pi_2'} F_\Lambda(L_2L_2'I_3I_2)\,\langle I_3\|\underset{\sim}{j}_N \underset{\sim}{A}_{L_2}^{(\pi_2)}\|I_2\rangle\langle I_3\|\underset{\sim}{j}_N \underset{\sim}{A}_{L_2'}^{(\pi_2')}\|I_2\rangle}{\sum_{L_2\pi_2}\langle I_3\|\underset{\sim}{j}_N \underset{\sim}{A}_{L_2}^{(\pi_2)}\|I_2\rangle^2} \qquad (8)$$

The F-coefficients $F_\Lambda(LL'I'I)$ are defined and tabulated in reference 33. It is useful to distinguish between the orientation coefficients $B_\Lambda(\gamma_1)$ which are characteristic of the (axially symmetric) orientation of the intermediate state I_2 and the directional distribution coefficients $A_\Lambda(\gamma_2)$ which characterize

the directional distribution of the gamma radiation γ_2 with respect to the orientation axis $\underset{\sim}{z}$ of the state I_2 ($\underset{\sim}{z}$ = propagation direction of γ_1) .

Most mixed multipole transitions are of the type E2 + M1. It is then convenient to introduce the "mixing ratio"

$$\delta(\gamma_n) = \frac{\langle I_{n+1} \| \underset{\sim}{j}_N \underset{\sim}{A}_2^{(E)} \| I_n \rangle}{\langle I_{n+1} \| \underset{\sim}{j}_N \underset{\sim}{A}_1^{(M)} \| I_n \rangle} = k_n \frac{\sqrt{3}}{10} \frac{\langle I_{n+1} \| \underset{\sim}{\gamma\gamma} (E2) \| I_n \rangle}{\langle I_{n+1} \| \underset{\sim}{\gamma\gamma} (M1) \| I_n \rangle} \tag{9}$$

where the initial state of the transition is written on the right side in the reduced matrix elements ($E_n > E_{n+1}$). The matrix elements and k_n in eq. (9) are expressed in units $\hbar = m = c = 1$.

The orientation parameter is then simply

$$B_\Lambda(\gamma_1) = (1 + \delta^2(\gamma_1))^{-1} (F_\Lambda(11\ I_1 I_2) - 2\,\delta(\gamma_1) F_\Lambda(12\ I_1 I_2) + \delta^2(\gamma_1) F_\Lambda(22\ I_1 I_2)) \tag{10}$$

and the directional distribution coefficient is

$$A_\Lambda(\gamma_2) = (1 + \delta^2(\gamma_2))^{-1} (F_\Lambda(11\ I_3 I_2) + 2\,\delta(\gamma_2) F_\Lambda(12\ I_3 I_2) + \delta^2(\gamma_2) F_\Lambda(22\ I_3 I_2)) \tag{11}$$

The mixing ratios defined in eq. (9) are related to those of Biedenharn and Rose[29] by

$$\delta(\gamma_1) = -\,\delta_{\text{Biedenharn-Rose}} \tag{12a}$$

$$\delta(\gamma_2) = \delta_{\text{Biedenharn-Rose}} \tag{12b}$$

The directional correlation of γ_1 with a gamma radiation γ_N, that follows some unobserved radiations $\gamma_2, \gamma_3, \ldots, \gamma_{N-1}$ which are emitted in cascade from the oriented state I_2 is given by

$$W(\theta) = \sum_\Lambda B_\Lambda(\gamma_1)\, U_\Lambda(\gamma_2)\, U_\Lambda(\gamma_3) \ldots\ldots U_\Lambda(\gamma_{N-1})\, A_\Lambda(\gamma_N)\, P_\Lambda(\cos\theta) \tag{13}$$

where the reorientation parameters $U_\Lambda(\gamma_n)$ for the n^{th} transition depend on I_n, I_{n+1} and on the multipole intensities L_n (but not the interference terms) of the unobserved radiation:

$$U_\Lambda(\gamma_n) = \frac{\sum_{L_n \pi_n} (-1)^{L_n} \begin{Bmatrix} I_n & I_n & \Lambda \\ I_{n+1} & I_{n+1} & L_n \end{Bmatrix} \langle I_{n+1} \| \underset{\sim}{j}_N \underset{\sim}{A}_{L_n}^{(\pi)} \| I_n \rangle^2}{\sum_{L_n \pi_n} (-1)^{L_n} \begin{Bmatrix} I_n & I_n & 0 \\ I_{n+1} & I_{n+1} & L_n \end{Bmatrix} \langle I_{n+1} \| \underset{\sim}{j}_N \underset{\sim}{A}_{L_n}^{(\pi)} \| I_n \rangle^2} \tag{14}$$

or for an unobserved E2 + M1 transition:

$$U_\Lambda(\gamma_n) = (-1)^{I_n + I_{n+1}} \left[(2I_n+1)\ (2I_{n+1}+1)\right]^{\frac{1}{2}} (1 + \delta(\gamma_n)^2)^{-1} \times \left[\delta^2(\gamma_n) \begin{Bmatrix} I_n & I_n & \Lambda \\ I_{n+1} & I_{n+1} & 2 \end{Bmatrix} - \begin{Bmatrix} I_n & I_n & \Lambda \\ I_{n+1} & I_{n+1} & 1 \end{Bmatrix}\right] \tag{15}$$

The reorientation coefficients of eqs. (14) and (15) are normalized to unity, i.e. $U_0(\gamma_n) = 1$.

In the present investigation only dipole and quadrupole radiations are involved. Hence the directional correlations are of the form:

$$W(\theta) = 1 + A_{22} P_2(\cos\theta) + A_{44} P_4(\cos\theta) \tag{16}$$

where the directional correlation coefficients $A_{\Lambda\Lambda}$ are given by

$$A_{\Lambda\Lambda} = B_\Lambda(\gamma_1)\, U_\Lambda(\gamma_2) \ldots\ldots U_\Lambda(\gamma_{N-1})\, A_\Lambda(\gamma_N) \tag{17}$$

Due to the finite size of source and detectors the experimentally observed directional correlation function is given by

$$W(\theta)' = A_{00}' + A_{22}' P_2(\cos\theta) + A_{44}' P_4(\cos\theta) \tag{18}$$

from which the theoretical correlation coefficients $A_{\Lambda\Lambda}$ can be extracted on the basis of

$$A_{\Lambda\Lambda} = \frac{A'_{\Lambda\Lambda}}{A'_{00}} \frac{1}{\bar{Q}_\Lambda(\gamma_1)\bar{Q}_\Lambda(\gamma_2)} \qquad (19)$$

where $\bar{Q}_\Lambda(\gamma_i) = Q_\Lambda(\gamma_i) / Q_0(\gamma_i)$ are the normalized geometrical correction coefficients for the detector that observes γ_i.

IV. EXPERIMENTAL PROCEDURE

For the γ-γ coincidence measurements, two coaxial Ge(Li) detectors (ORTEC, 30 cc) having a resolution of 3 keV for Ni^{60} γ-rays were employed. A block diagram of the coincidence electronics used for the direct γ-γ measurements[34] is shown in Fig. 2. Four single channel analyzers were used to perform the energy selection for each detector; two single channel analyzers were set on the output of the time-to-amplitude converter. In this way both true and accidental coincidences could be simultaneously measured for up to four coincidence configurations. The effective resolving time of the coincidence circuit was approximately 50 nsec.

For the measurement of coincidence spectra (indirect γ-γ measurement), the entire gamma spectrum was accepted by one of the single channel analyzers; the output of the appropriate coincidence module was used to gate the multichannel analyzer. This left three coincidence modules available for direct γ-γ measurements.

In the direct γ-γ measurement, singles and coincidence data were accumulated for fixed time intervals in an automatic angular correlation apparatus. After normalization for variations in the singles counting rates and for source decay, the data were fitted to eq. (18) by the method of least squares. The results were then corrected for finite detector angular resolution and finite source dimension according to eq. (19), using correction factors which were calculated as described below.

The geometrical correction factors $\bar{Q}_\Lambda(\gamma_i)$ constitute a significant part of the analysis of directional correlation results. For coaxial Ge(Li) detectors and source distances of a few centimeters, the product $\bar{Q}_\Lambda(\gamma_1)\bar{Q}_\Lambda(\gamma_N)$ may give rise to a 10% correction for $\Lambda = 2$ and a 25% correction for $\Lambda = 4$. Thus a careful determination of the appropriate $\bar{Q}_\Lambda(\gamma_i)$ is called for. In the present case, these factors were measured using positron annihilation radiation.[35] The resulting factors were checked with the $4^+ - 2^+ - 0^+$ directional correlation in Ni^{60} and the $0^+ - 2^+ - 0^+$ directional correlation in Pd^{106}. In addition, calculations of the $\bar{Q}_\Lambda(\gamma_i)$ have been made using the NaI(Tl) method of Rose[36] adapted to coaxial Ge(Li) detectors[37], and also using the Monte Carlo method[38]. The results of these calculations are in excellent agreement with the measured values, and in addition demonstrate that the dependence of the $\bar{Q}_\Lambda(\gamma_i)$ on the gamma-ray energy can be neglected within the range of gamma energies encountered in our measurements. Due to the short lifetimes of the excited states involved, no corrections for external perturbations were expected; none was observed to be necessary.

In the case of the coincidence spectra measurements, the data were summed over all channels comprising the peak in the multichannel analyzer spectrum. A reasonable estimate was made for the background under the peak, which was assumed to be linear; this was then subtracted from the data. This method was judged superior to fitting the peaks to a Gaussian shape function; the Gaussian method yielded the same results for the lines of high intensity as the summing

method, but was not as good for fitting the weaker lines. The method of integrating the intensity of each line proved more successful than fitting the data channel-by-channel, since it minimized effects due to electronic instability of the linear analysis circuitry. A separately measured chance coincidence spectrum was used to correct for chance coincidence effects. The integrated peak intensities at the various angles were fitted to eq. (18) by the method of least squares, with the appropriate normalization and geometrical correction factors applied as described above.

A liquid source consisting of $AgNO_3$ in dilute HNO_3 was used for the directional correlation measurements of the Cd^{110} gamma rays. The source, of roughly 15 μc activity, was placed in a thin-walled glass ampule of approximately 2 mm diameter and 8 mm length. Due to the long half-life of the source (253 days), it was not necessary to accumulate peak and background spectra simultaneously; hence the full range of the multichannel analyzer could be used for each measurement, and optimum resolution conditions could be obtained. The singles gamma spectrum of the Cd^{110} gamma rays is shown in Fig. 3.

Spectra were accumulated in coincidence with each of the four most intense transitions observed in the Ag^{110m} decay - (658 keV, 764 keV, 885 keV, 937 keV). All except the 885 keV line were measured at three angles (90°, 135°, 180°); the 885 keV line was used as a calibration measurement and was measured at only two angles (90°, 180°). Hence only the correlation anisotropy may be extracted from measurements gated on the 885 keV line.

In most direct γ-γ angular correlation measurements, the energy region accepted for each γ-ray also includes a background due to Compton-scattered photons from higher energy γ-rays. These photons give rise to spurious coincidences having in general different angular distributions than the cascade under

investigation. Such coincidences result in two first order effects on the measured correlation, caused by coincidences between one gamma ray and the background under the other. There is also a second order effect caused by coincidences between the two Compton backgrounds, which can in most cases be neglected; however, for weak γ-rays, the second order effect can be larger than the first order.

In general, then, at least three measurements are required for an unambiguous analysis of a γ-γ directional correlation. One must measure coincidences between the two gamma rays, including their respective Compton backgrounds, and also between each gamma ray and the Compton background below the other. This requires that each gamma ray have a flat background, and that it be isolated enough from other γ-rays to make that background accessible; these conditions are seldom met in practice.

These difficulties can in part be overcome by the indirect γ-γ correlation method. One gamma ray is measured in coincidence with an entire gamma spectrum; the results of measurements at several angles are stored in a multichannel analyzer. The resulting coincidence spectra are examined to determine the intensities of the peaks above the background. This not only allows one to separate a peak from the background below it, but also to examine simultaneously several different peaks. By making measurements gating first on a gamma peak and then on the background represented in an energy region slightly above or below that peak, the correlation data, free of any interfering Compton background effects, can be measured. This requires that only one line have a flat and accessible Compton background, and thus allows a wider range of measurements to be made.

An example of the necessity of measuring such corrections is given by the measurements of the 937 keV - 885 keV cascade in Cd^{110}. Both lines are of high

intensity and one would expect that the interfering effects of the Compton background would be small. However, a direct γ-γ correlation measurement yielded the result

$$A_{22} = 0.055 \pm 0.010 \ .$$

This is not in agreement with the expected result for the $6^+ - 4^+ - 2^+$ spin sequence ($A_{22} = 0.102$). In order to explain the low measured value, it is necessary to consider only an admixture of 10% of the 1384 keV - 885 keV correlation ($A_{22} = -.284$), with the energy region accepted for the 937 keV line including Compton events due to the 1384 keV transition. The result of the indirect coincidence spectrum measurement, after making corrections for background effects, was

$$A_{22} = 0.098 \pm 0.010 \ ,$$

in good agreement with the expected value, $A_{22} = 0.102$.

A dramatic illustration of the effects of background corrections on coincidence spectra is provided by the spectra shown in Fig. 4. Part (a) shows a spectrum taken in coincidence with the 658 keV ($2^+ \rightarrow 0^+$) transition. Note the strong presence of the 658 keV line in the spectrum, due to the presence in the gating energy region of background events of transitions which are in coincidence with the 658 keV line. Part (b) shows the effect of these background events only; the spectrum is obtained by gating on an energy region slightly lower than the 658 keV line. Here we see the strong presence of the 658 keV line. Part (c) shows the difference between (a) and (b). Now the 658 keV line has almost disappeared, demonstrating the extreme care that must be taken in analyzing γ-γ coincidence results obtained from Ge(Li) detector measurements.

V. RESULTS

The results for the directional correlation coefficients A_{22} and A_{44} extracted from the indirect angular correlation measurements are given in Table I. The quoted errors are mainly caused by the uncertainties associated with the Compton background subtraction (about 5 percent).

The directional correlation coefficients A_{22} and A_{44} obtained from direct angular correlation measurements are given in Table II. The first three entries are for cascades in which the contributions due to the Compton background are expected to be small; the last entry was derived by measuring the directional correlation of the Compton background both above and below the 818 keV line and by applying these results to the analysis of the directly measured 818 keV - 658 keV directional correlation.

The results given in Tables I and II show a high degree of internal consistency, with overlap well within the expected error limits. Indirect directional correlation measurements involving any two members of the $\gamma_{11} - \gamma_{10} - \gamma_3$ cascade (6^+-4^+-2^+-0^+) yield the expected coefficient $A_{22} = 0.102$. In addition, all three of these transitions are in coincidence with γ_1; the three results for measurements involving γ_1 agree quite well. In general, good agreement is obtained between the results of the direct and indirect methods.

The E2/M1 mixing ratios $\delta(\gamma_n)$ were obtained from either eq. (10) or eq. (11) depending on whether the gamma transition γ_n was the first or second radiation emitted in the gamma-gamma cascade under consideration.

The observed coefficients $A_{\Lambda\Lambda}$ for 1 - 3 and 1 - 4 directional correlations must be analyzed in terms of several factors as given in eq. (17). In most cases there are unknown mixing parameters involved in the $U_\Lambda(\gamma_n)$ as well

as in the $B_A(\gamma_1)$ or the $A_A(\gamma_N)$. Thus an unambiguous analysis to determine all unknown values of the mixing parameter $\delta(\gamma_n)$ is impossible. However, the indirect directional correlation method resolves the difficulty at once. If a given measurement includes the cascade γ_1-γ_2-γ_3 taken in coincidence with the pure γ_3, then the γ_2-γ_3 analysis will yield the correct value for $\delta(\gamma_2)$, which leads to the value of $U_A(\gamma_2)$ that is required to analyze the γ_1-γ_3 correlation and to extract $\delta(\gamma_1)$. If γ_1 is a pure multipole transition this method provides two independent determinations of $\delta(\gamma_2)$. Many of the Cd^{110} gamma transitions were involved in several of the gamma-gamma directional correlation measurements either as a first, second or intermediate (unobserved) transition. Hence in many cases the mixing ratio of a particular transition could be extracted from several independent measurements, and the results could be checked for internal consistencies.

The values of the E2/M1 mixing ratios $\delta(\gamma_n)$ are tabulated in Table III. The $\delta(\gamma_n)$ are defined in eq. (9). The mixing amplitude ratios $\Delta(\gamma_n)$ in terms of the Bohr-Mottelson reduced matrix elements

$$\Delta(\gamma_n) = \frac{\langle I_{n+1} \| \mathcal{M}(E2) \| I_n \rangle}{\langle I_n \| \mathcal{M}(M1) \| I_n \rangle} \qquad (20)$$

where the multipole moments are expressed in natural units ($\hbar$ = m (electron mass) = c = 1) are given in column four of Table III.

Frequently, the E2 multipole moments are given in units of (e x b) ($b = 10^{-24} cm^2$) and the M1 multipole moments are expressed in terms of the nuclear magneton $\mu_N = e\hbar/2Mc$. The ratios $\Delta(\gamma_n)$ in units of $(e \times b)/\mu_N$ are listed in column five of Table III. All mixing ratios have been extracted from at least three independent measurements. The analysis of the numerous A_{22} and A_{44} data in terms of the mixing ratios δ resulted in a completely consistent

set of δ data.

As a by-product of the analysis of the directional correlation data, all previously assumed spin assignments[20,21] for the excited states of Cd^{110} have been verified, and a definite spin-parity assignment of 4^+ could be made to 2219.9 keV state.

Fig. 5 shows the excited states and the gamma transition of Cd^{110}. The relative intensity of the M1 components in the mixed E2 - M1 transitions are indicated in brackets (in percent of the total E2 + M1 intensity).

VI. DISCUSSION

The mixing ratios of the 1384 keV and the 1505 keV gamma transition have been measured before with NaI(Tl) scintillation detectors[13,14,19]. Our results are in good agreement with the most recent of these measurements[19] (taking into account the different definitions of δ !). The mixing ratio of the 818 keV gamma transition has been measured by Milner et al.[23] in Coulomb excitation experiments. Their result $\delta = -1.5$ is in fair qualitative agreement with our result $\delta = -1.20 \pm 0.15$.

The mixing ratios extracted from the γ-γ directional correlation measurements are consistent with the K-conversion coefficients which were obtained by Hagues et al.[20]. Unfortunately, the K-conversion coefficients are not strongly dependent on the relative amount of the M1 and E2 intensities for Z = 48 and for k = 0.7 ($\approx$ 360 keV). Hence the K-conversion data are not very useful for an independent determination of the E2/M1 mixing ratio.

It is interesting to note that all gamma transitions in Cd^{110} for which the angular momentum selection rules allow the emission of M1 radiation ($\Delta I = 0, \pm 1$), contain a sizeable amount of the M1 component. It is also

noteworthy that the relative phases of the E2 and M1 reduced matrix elements in all mixed transitions of Cd^{110} are the same. There is no pronounced systematic trend of the amount of M1 admixture as one goes to higher excited states. One might expect a larger M1 admixture in the transitions between higher excited states which are expected to conform less to the vibrational picture. In fact, the smallest M1 admixture is found in the 818 keV gamma transition from the "two-phonon" 2^+ state to the one-phonon 2^+ state. However, the intensity of the M1 component (41 percent) is still large and in clear disagreement with the predictions of the simple vibrational model.

TABLE I. Results for the Directional Correlation Coefficients Extracted from the Indirect Correlation Measurements on the Cd^{110} Gamma Transitions

Gamma Ray Energy (keV)	Gating Transition			
	γ_3 658 keV	γ_8 764 keV	γ_{10} 885 keV	γ_{11} 937 keV
γ_1 447	A_{22}= .23 ± .20 A_{44}= - .01 ± .29		A_{22}= .21 ± .22	A_{22}= .20 ± .15 A_{44}= .02 ± .18
γ_2 620	A_{22}= .42 ± .40 A_{44}= - .18 ± .59	A_{22}= .040 ± .105 A_{44}= -.050 ± .103	A_{22}= .40 ± .15	
γ_3 658		A_{22}= .050 ± .028 A_{44}= .001 ± .035	A_{22}= .102 ± .011	A_{22}= .097 ± .025 A_{44}= .025 ± .035
γ_4 678	A_{22}= .250 ± .091 A_{44}= -.066 ± .120		A_{22}= .241 ± .046	
γ_5 687	A_{22}= - .06 ± .26 A_{44}= .03 ± .34	A_{22}= -.233 ± .050 A_{44}= -.094 ± .065		
γ_6 707	A_{22}= -.283 ± .080 A_{44}= -.076 ± .133		A_{22}= -.339 ± .050	
γ_7 744	A_{22}= .10 ± .40 A_{44}= - .07 ± .54			
γ_8 764	A_{22}= .064 ± .040 A_{44}= -.027 ± .043		A_{22}= -.073 ± .102	
γ_9 818	A_{22}= .481 ± .082 A_{44}= .155 ± .112	A_{22}= .032 ± .050 A_{44}= .018 ± .056		
γ_{10} 885	A_{22}= .098 ± .013 A_{44}= .016 ± .016	A_{22}= .201 ± .100 A_{44}= .018 ± .130		A_{22}= .102 ± .016 A_{44}= .028 ± .020
γ_{11} 937	A_{22}= .102 ± .018 A_{44}= .015 ± .025		A_{22}= .098 ± .010	
γ_{12} 1384	A_{22}= -.308 ± .020 A_{44}= -.018 ± .026		A_{22}= -.292 ± .012	
γ_{13} 1476		A_{22}= .017 ± .060 A_{44}= .095 ± .078		
γ_{14} 1505	A_{22}= -.471 ± .010 A_{44}= -.040 ± .020	A_{22}= -.178 ± .026 A_{44}= -.047 ± .033		
γ_{15} 1562	A_{22}= .120 ± .050 A_{44}= .040 ± .060			

TABLE II. Results for the Directional Correlation Coefficients Extracted from the Direct Correlation Measurements on the Cd^{110} Gamma Transitions

γ - γ Cascade	A_{22}	A_{44}
1505 - 658	-0.403 ± 0.014	-0.027 ± 0.020
764 - 1505	-0.184 ± 0.024	-0.031 ± 0.037
1384 - 885	-0.281 ± 0.013	-0.010 ± 0.019
818 - 658	0.375 ± 0.050	0.180 ± 0.050

TABLE III. The E2/M1 Mixing Ratios of the Cd^{110} Gamma Transitions

Gamma Transition keV	$\Delta I = I_i - I_f$	$\delta(\gamma_n) = \frac{\langle I_{n+1}\|\|_{j\ldots N} A_{\ldots 2}^{E}\|I_n\rangle}{\langle I_{n+1}\|\|_{j\ldots N} A_{\ldots 1}^{M}\|I_n\rangle}$	$\Delta(\gamma_n) = \frac{\langle I_{n+1}\|\|\gamma\ell\,(E2)\|I_n\rangle}{\langle I_{n+1}\|\|\gamma\ell\,(M1)\|I_n\rangle}$ (In natural units)	$\Delta(\gamma_n) = \frac{\langle I_{n+1}\|\|\gamma\ell\,(E2)\|I_n\rangle(\text{in e x b})}{\langle I_{n+1}\|\|\gamma\ell\,(M1)\|I_n\rangle(\text{in n. m.})}$
446.7	-1	- 0.45 ± 0.20	- 3.0 ± 1.3	- 1.2 ± 0.5
620.2	-1	- 0.80 ± 0.50	- 3.8 ± 2.4	- 1.55 ± 0.95
657.7	+2	∞	∞	∞
677.5	0	- 0.25 ± 0.20	- 1.09 ± 0.88	- 0.44 ± 0.36
686.8	+1	- 1.1 $^{+\ 0.8}_{-\ 0.4}$	- 4.7 $^{+\ 3.4}_{-\ 1.7}$	- 1.9 $^{+\ 1.4}_{-\ 0.7}$
706.7	+1	- 1.0 ± 0.3	- 4.2 ± 1.3	- 1.7 ± 0.5
744.2	+2	∞	∞	∞
763.9	+2	∞	∞	∞
818.0	0	- 1.20 ± 0.15	- 4.3 ± 0.5	- 1.75 ± 0.22
884.7	+2	∞	∞	3
937.5	+2	∞	∞	∞
1384.2	+1	- 0.37 ± 0.03	- 0.79 ± 0.06	- 0.32 ± 0.03
1475.7	+2	∞	∞	∞
1504.9	+1	- 0.55 ± 0.10	- 1.08 ± 0.20	- 0.44 ± 0.08
1562.2	+2	∞	∞	∞

REFERENCES

* Work supported by the U. S. Atomic Energy Commission under Contract No. AT(11-1)1746 (Chicago Operations Office)

† NASA - Fellow

1. G. S. Goldhaber and J. Weneser, Phys. Rev. 98, 212 (1955).
N. MacDonald, Nucl. Phys. 48, 500 (1963).
2. L. Wilets and M. Jean, Phys. Rev. 102, 788 (1956).
3. J. de Boer, R. G. Stokstad, G. D. Symons, and A. Winther, Phys. Rev. Letters 14, 564 (1965).
J. J. Simpson, D. Eccleshall, M. J. L. Yates, and N. J. Freeman, Nucl. Phys. A94, 177 (1967).
R. G. Stokstad, I. Hall, G. D. Symons, and J. de Boer, Nucl. Phys. A92 319 (1967).
P. H. Stelson, W. T. Milner, J. L. C. Ford, Jr., F. K. McGowan, and R. L. Robinson, Bull. Am. Phys. Soc. 10, 427 (1965).
G. R. Schilling, R. P. Scharenberg, and J. W. Tippie, Phys. Rev. Letters 19, 318 (1967).
J. E. Glenn and J. X. Saladin, Phys. Rev. Letters 19, 33 (1967).
J. X. Saladin, J. E. Glenn, and J. Pryor, Phys. Rev. 186, 1241 (1969).
G. R. Schilling, R. P. Scharenberg, and J. W. Tippie, Phys. Rev. (to be published).
4. T. Tamura and T. Udagawa, Phys. Rev. 150, 783 (1966).
5. D. R. Bès, G. G. Dussel and J. Gratton, Proc. Int. Nucl. Phys. Conf., R. L. Becker, Ed. (Academic Press, New York 1967), p. 598.
6. B. Sorensen, Proc. Int. Nucl. Phys. Conf., R. L. Becker, Ed. (Academic Press, New York 1967), p. 580.

7. B. Sorensen, Phys. Letters 21, 683 (1966).
8. B. R. Mottelson, J. Phys. Soc. Japan 28 (Suppl.), 87 (1968)
9. A. M. Korolev, Izv. Akad. Nauk SSSR, Ser. Fiz. 31, 1701 (1967). Trans., Bull Acad. Sci. USSR Phys. Ser. 31, 1740 (1967).
10. K. Kumar and M. Baranger, Nucl. Phys. 92, 608 (1967) ibid A122, 273 (1968), Phys. Rev. Letters 17, 1146 (1966).
11. K. Kumar, Phys. Letters 29B, 25 (1969).
12. A. C. Knipper, Proc. Phys. Soc. 71, 77 (1958).
13. E. G. Funk, Jr., and M. L. Wiedenbeck, Phys. Rev. 112, 1247 (1958).
14. H. W. Taylor and W. R. Frisken, Phys. Rev. 114, 127 (1959).
15. H. W. Taylor and S. A. Scott, Phys. Rev. 114, 121 (1959).
16. T. Katoh and Y. Yoshizawa, Nucl. Phys. 32, 5 (1962).
17. J. Schintlmeister and L. Werner, Nucl. Phys. 51, 383 (1964).
18. W. B. Newbolt and J. H. Hamilton, Nucl. Phys. 53, 353 (1964).
19. F. Münnich, K. Fricke, and J. Koch, Z. Phys. 181, 301 (1964).
20. J. A. Moragues, P. Reyes-Suter, and T. Suter, Nucl. Phys. A99, 652 (1967).
21. S. M. Brahmavar, J. H. Hamilton, and A. V. Ramayya, Nucl. Phys. A125, 217 (1969).
22. M. Koike et al., Nucl. Phys. A125, 161 (1969).
23. W. T. Milner, F. K. McGowan and P. H. Stelson, Nucl. Phys. (to be published).
24. J. R. Van Hise, M. C. Kelley, R. G. Lanier and N. R. Johnson, Phys. Rev. (to be published).
25. L. Keszthelyi, I. Demeter, I. Dézsi and L. Varga, Hyperfine Structure and Nuclear Radiation, E. Matthias and D. A. Shirley, Eds., (North-Holland Publishing Co., Amsterdam 1968), p. 155.
26. K. Kumar, Phys. Rev. (to be published).
27. R. Beyer, R. P. Scharenberg and J. Thomson, Phys. Rev. (to be published).

28. P. H. Stelson, quoted in J. de Boer and J. Eichler, Advances in Nuclear Physics, M. Baranger and E. Vogt, Eds. (Plenum Press, Inc., New York, 1968) Vol. I, p. 1.

29. L. C. Biedenharn and M. E. Rose, Revs. Mod. Phys. 25, 729 (1953).

30. H. J. Rose and D. M. Brink, Revs. Mod. Phys. 39, 306 (1967).

31. A. Bohr and B. R. Mottelson, Nuclear Structure, Vol. I (W. A. Benjamin, Inc., New York, 1969) p. 381.

32. K. Alder et al., Revs. Mod. Phys. 28, 432 (1956).

33. H. Frauenfelder and R. M. Steffen, in Alpha- Beta- and Gamma-Ray Spectroscopy, K. Siegbahn, Ed. (North-Holland Publishing Co., Amsterdam 1965), p. 997.

34. For purpose of reference, the term "direct" γ-γ measurement will refer to one in which a single γ-ray is measured in cascade with another γ-ray and the number of coincidences is counted; an "indirect" measurement will refer to one in which the coincidence data is extracted from a gated energy spectrum of coincidence counts.

35. E. L. Church and J. J. Kraushaar, Phys. Rev. 88, 419 (1952).

36. M. E. Rose, Phys. Rev. 91, 610 (1953).

37. F. T. Avignone III and G. D. Frey, Rev. Sci. Instr. 39, 1941 (1968) and 40, 1365 (1969).

38. D. C. Camp and A. L. Van Lehn, Nucl. Instr. and Meth. 76, 192 (1969).

FIGURE CAPTIONS

Fig. 1. Excited States of Cd^{110}

Fig. 2. Block Diagram of Plural Channel Coincidence Electronics

Fig. 3. Gamma Spectrum of Ag^{110m} - Cd^{110} Observed with a 30 cc Ge(Li) Detector

Fig. 4. Spectrum of the Cd^{110} Gamma Rays in Coincidence with the 658 keV Transition

a) Coincidence Spectrum Observed with the Gate-window on the 658 keV Peak

b) Coincidence Spectrum Observed with the Gate-window below the 658 keV Peak

c) Coincidence Spectrum Corrected for the Compton Background under the 658 keV Peak

Fig. 5. Decay Scheme of Ag^{110m} - Cd^{110} Including the M1 Admixture (in percent of the total M1 + E2 intensity) to the Various Mixed Multipole Transitions

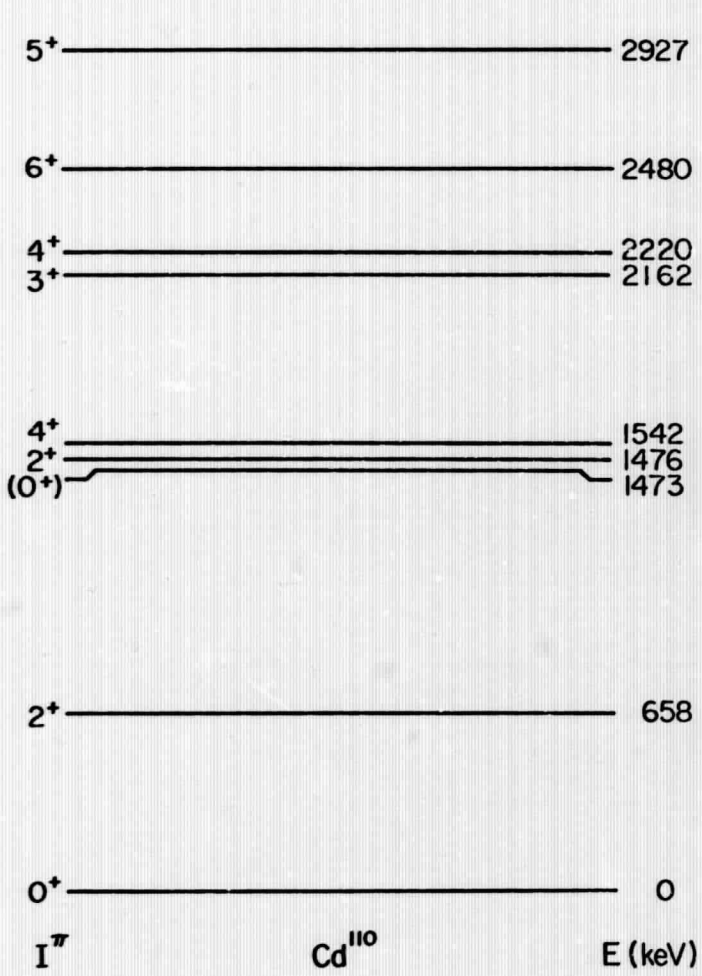
5+
2927
6+
2480
4+
2220
3+
2162
4+
1542
2+
1476
(0+)
1473
2+
658
0+
0
I^π
Cd^110
E (keV)

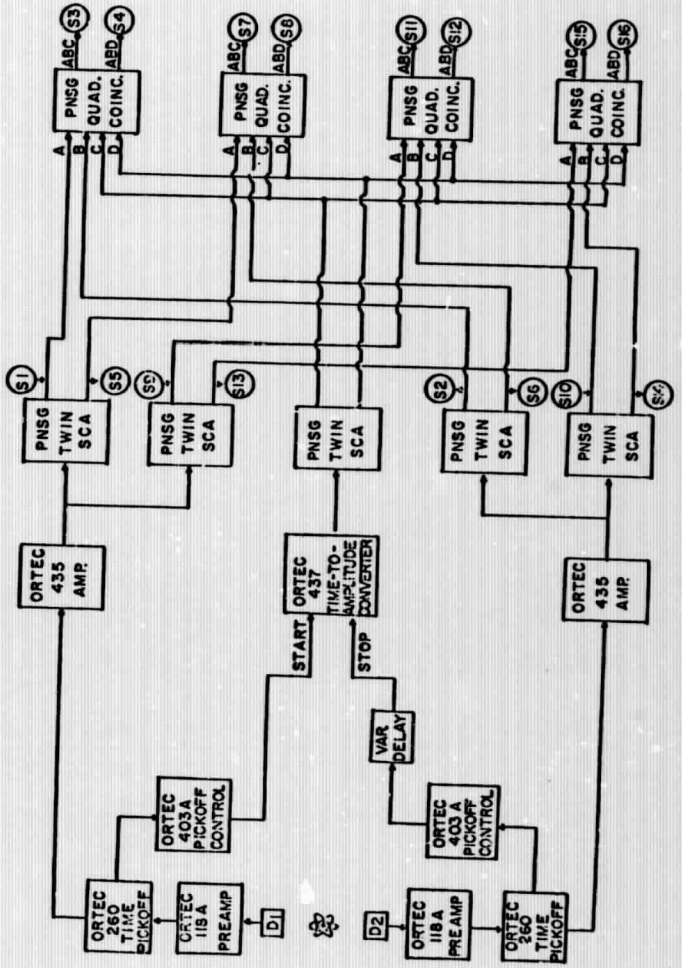
PNSG QUAD. COINC.
ABC
ABD
A
B
C
D
S1
S2
S3
S4
S5
S6
S7
S8
S9
S10
S11
S12
S13
S14
S15
S16
PNSG TWIN SCA
ORTEC 435 AMP.
ORTEC 437 TIME-TO-AMPLITUDE CONVERTER
START
STOP
VAR DELAY
ORTEC 403A PICKOFF CONTROL
ORTEC 260 TIME PICKOFF
ORTEC 118A PREAMP
D1
D2

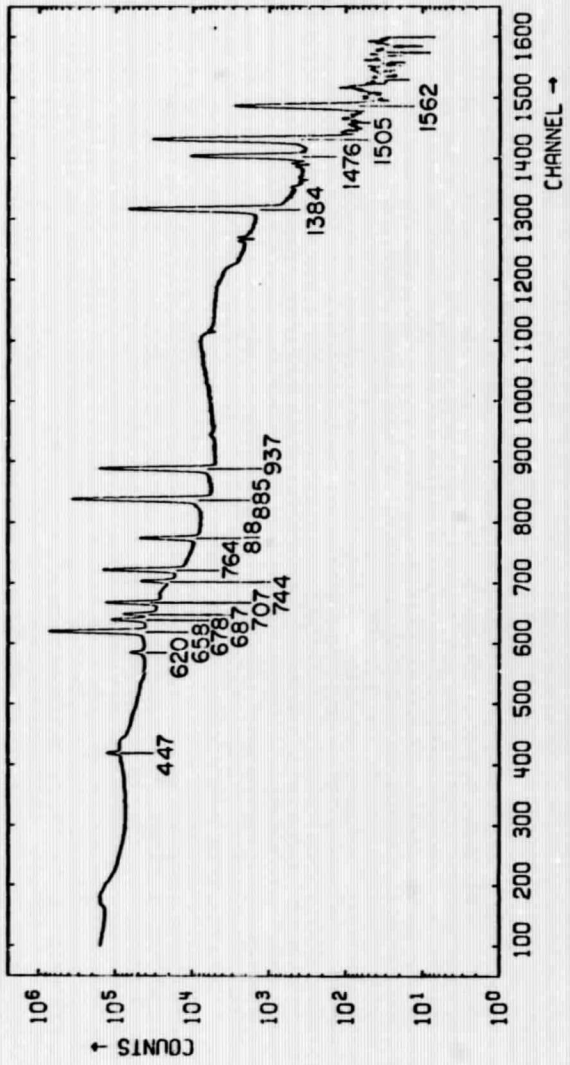
COUNTS →
CHANNEL →
447
620
658
678
687
707
744
764
818
885
937
1384
1476
1505
1562

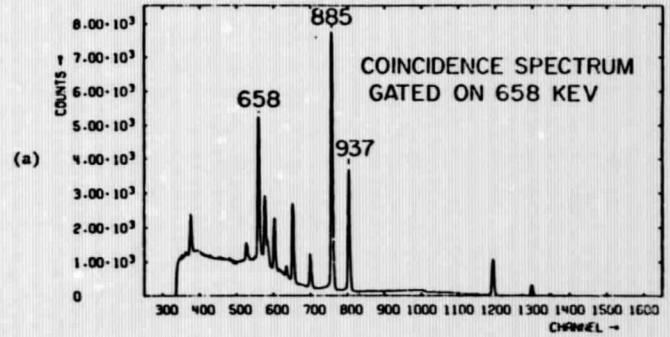
(a)
COINCIDENCE SPECTRUM
GATED ON 658 KEV
658
885
937
COUNTS →
CHANNEL →

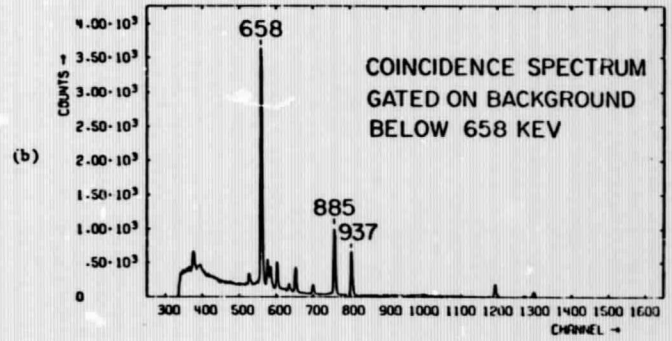
(b)
COINCIDENCE SPECTRUM
GATED ON BACKGROUND
BELOW 658 KEV
658
885
937
COUNTS →
CHANNEL →

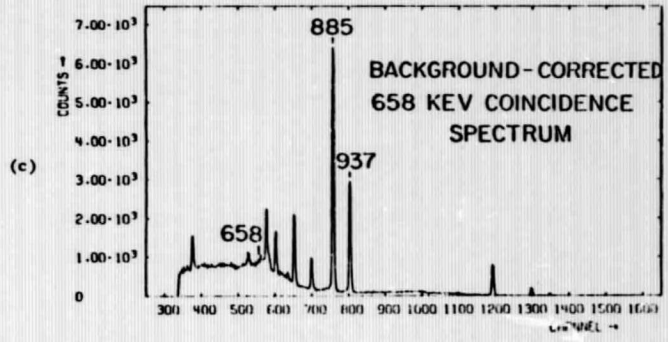
(c)
BACKGROUND-CORRECTED
658 KEV COINCIDENCE
SPECTRUM
658
885
937
COUNTS →

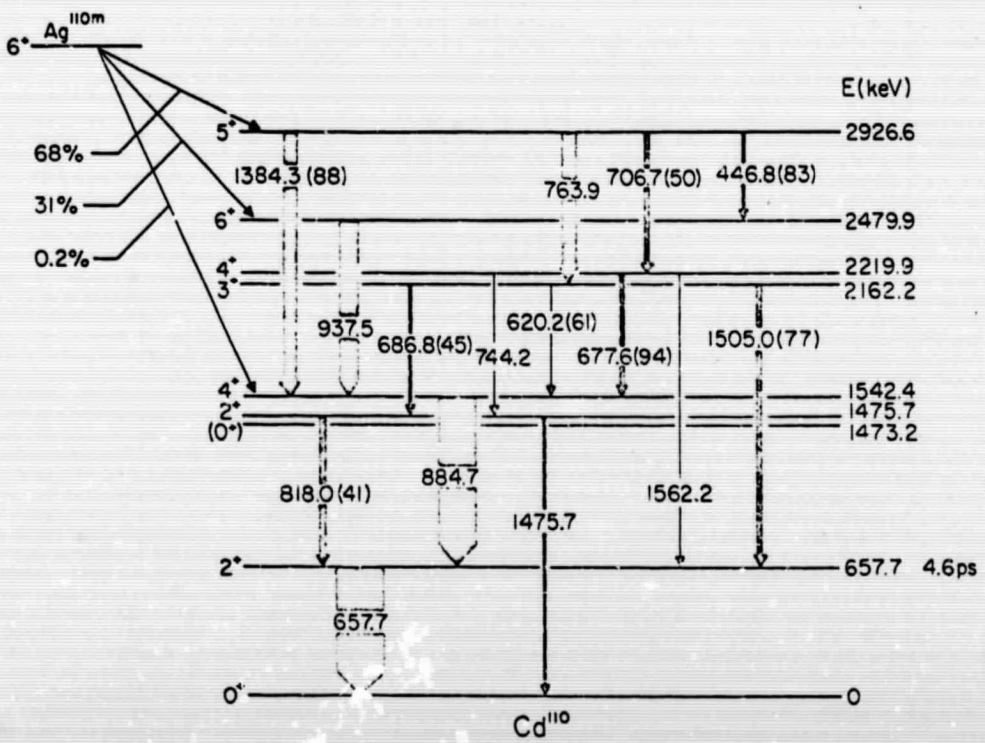
6+
Ag110m
68%
31%
0.2%
E(keV)
5+
2926.6
1384.3 (88)
763.9
706.7(50)
446.8(83)
6+
2479.9
4+
3+
2219.9
2162.2
937.5
686.8(45)
744.2
620.2(61)
677.6(94)
1505.0(77)
4+
2+
(0+)
1542.4
1475.7
1473.2
818.0(41)
884.7
1562.2
1475.7
2+
657.7 4.6ps
657.7
0+
0
Cd110